5772 *Chem. Mater.* **2009,** *21,* 5772–5782
DOI:10.1021/cm902013k

CHEMISTRY OF MATERIALS
Article

Structure and Dynamics for $LiBH_4$−LiCl Solid Solutions

Lene M. Arnbjerg,[†] Dorthe B. Ravnsbæk,[†] Yaroslav Filinchuk,[‡] Ronnie T. Vang,[§] Yngve Cerenius,[∥] Flemming Besenbacher,[§] Jens-Erik Jørgensen,[†] Hans Jørgen Jakobsen,[⊥] and Torben R. Jensen*,[†]

[†]*Interdisciplinary Nanoscience Center (iNANO) and Department of Chemistry, Aarhus University, Building 1512, DK-8000 Aarhus C, Denmark,* [‡]*Swiss-Norwegian Beamlines at the ESRF, 6 rue Jules Horowitz, 38043 Grenoble Cedex, France,* [§]*Interdisciplinary Nanoscience Center (iNANO) and Department of Physics and Astronomy, Aarhus University, Building 1521 DK-8000 Aarhus C, Denmark,* [∥]*MAXLAB, Lund University, S-22100 Lund, Sweden, and* [⊥]*Instrument Centre for Solid-State NMR Spectroscopy and Interdisciplinary Nanoscience Center (iNANO), Aarhus University, Langelandsgade 140, DK-8000 Aarhus C, Denmark*

Received July 6, 2009. Revised Manuscript Received October 24, 2009

A surprisingly high degree of structural and compositional dynamics is observed in the system $LiBH_4$−LiCl as a function of temperature and time. Rietveld refinement of synchrotron radiation powder X-ray diffraction (SR-PXD) data reveals that Cl^- readily substitutes for BH_4^- in the structure of $LiBH_4$. Prolonged heating a sample of $LiBH_4$−LiCl (1:1 molar ratio) above the phase transition temperature and below the melting point ($108 < T < 275$ °C) can produce highly chloride substituted hexagonal lithium borohydride, h-$Li(BH_4)_{1-x}Cl_x$, e.g., $x \sim 0.42$, after heating from room temperature (RT) to 224 °C at 2.5 °C/min. LiCl has a higher solubility in h-$LiBH_4$ as compared to orthorhombic lithium borohydride, o-$LiBH_4$, which is illustrated by a $LiBH_4$−LiCl (1:1) sample equilibrated at 245 °C for 24 days and left at RT for another 13 months. Rietveld refinement reveals that this sample contains o-$Li(BH_4)_{0.91}Cl_{0.09}$ and LiCl. This illustrates a significantly faster dissolution of LiCl in h-$LiBH_4$ as compared to a slower segregation of LiCl from o-$LiBH_4$, which is also demonstrated by in situ SR-PXD from three cycles of heating and cooling of the same $Li(BH_4)_{0.91}Cl_{0.09}$ sample. The substitution of the smaller Cl^- for the larger BH_4^- ion is clearly observed as a reduction in the unit cell volume as a function of time and temperature. A significant stabilization of h-$LiBH_4$ is found to depend on the degree of anion substitution. Variable temperature solid-state magic-angle spinning (MAS) ^{7}Li and ^{11}B NMR experiments on pure $LiBH_4$ show an increase in full width at half maximum (fwhm) when approaching the phase transition from o- to h-$LiBH_4$, which indicates an increase of the relaxation rate (i.e., T_2 decreases). A less pronounced effect is observed for ion-substituted $Li(BH_4)_{1-x}Cl_x$, $0.09 < x < 0.42$. The MAS NMR experiments also demonstrate a higher degree of motion in the hexagonal phase, i.e., fwhm is reduced by more than a factor of 10 at the o- to h-$LiBH_4$ phase transition.

1. Introduction

The use of hydrogen (H_2) as an energy carrier in a future hydrogen society may form the basis of a more environmentally friendly and carbon free energy system. The Achilles heel in this scenario, which utilizes a variety of renewable energy sources to produce hydrogen as an energy carrier for mobile applications (e.g., cars), is the development of an efficient, lightweight, compact, robust, safe, and low-priced method for the storage of hydrogen. This may be realized through solid-state H_2 storage.[1−3] This has prompted significant research within the light-element hydrides during the past decade, in particular for complex hydrides based on BH_4^-, NH_2^-/NH^{2-}, and AlH_4^-/AlH_6^{3-}.[4−8]

Obviously, lithium borohydride ($LiBH_4$) has great potential as a possible future hydrogen storage medium and has received much interest due to high gravimetric and volumetric hydrogen storage capacity of $\rho_m = 18.5$ wt % and $\rho_V = 121$ kg H_2 m^{-3}, respectively.[9,10] At room temperature, $LiBH_4$ exists as an orthorhombic phase, denoted as o-$LiBH_4$ (space group *Pnma*) that undergoes a first-order phase transition to a hexagonal phase, denoted h-$LiBH_4$ ($P6_3mc$) at ca. 108 °C, with a melting point reported to be 275 °C.[9,10] The structures of the two

*Corresponding author. E-mail address: trj@chem.au.dk. Phone: +45 8942 3894. Fax: +45 8619 6199.

(1) Schlapbach, L.; Züttel, A. *Nature* **2001**, *414*, 353–358.
(2) Züttel, A. *Naturwissenschaften* **2004**, *91*, 157–172.
(3) Ritter, J. A.; Ebner, A. D.; Wang, J.; Zidan, R. *Mater. Today* **2003**, No. Sept, 18–23.
(4) Felderhoff, M.; Weidenthaler, C.; von Helmolt, R.; Eberle, U. *Phys. Chem. Chem. Phys.* **2007**, *9*, 2643–2653.
(5) Grochala, W.; Edwards, P. P. *Chem. Rev.* **2004**, *104*, 1283–1315.
(6) Orimo, S.; Nakamori, Y.; Eliseo, J. R.; Zuttel, A.; Jensen, C. M. *Chem. Rev.* **2007**, *107*, 4111–4132.
(7) Filinchuk, Y.; Chernyshov, D.; Dmitriev, V. *Z. Kristallogr.* **2008**, *223*, 649–659.
(8) Hauback, B. C. *Z. Kristallogr.* **2008**, *223*, 636–648.
(9) Soulié, J.-Ph.; Renaudin, G.; Černý, R.; Yvon, K. *J. Alloys Compd.* **2002**, *346*, 200–205.
(10) Züttel, A.; Rentsch, S.; Fischer, P.; Wenger, P.; Sudan, P.; Mauron, Ph.; Emmenegger, Ch. *J. Alloys Compd.* **2003**, *356−357*, 515–520.

 Published on Web 11/18/2009

polymorphs of lithium borohydride have originally been investigated by powder X-ray diffraction (PXD),[9,10] but recently also by single-crystal X-ray diffraction, neutron diffraction, and theoretical methods.[11−14] Unfortunately, this material suffers from poor thermodynamics, i.e., high enthalpy of decomposition $\Delta H = -68.9$ kJ/mol, and hydrogen release therefore occurs at a relatively high temperature ($T > 300$ °C).[15] On the other hand, $LiBH_4$ in its molten state is very reactive and also reacts with gold.[16] This ability has been utilized in the design of reactive hydride composites (RCH), e.g., the system $2LiBH_4-MgH_2$, which has an enthalpy of decomposition of only −42 kJ/mol and is still capable of storing 11.5 wt % H_2.[17,18] Self-catalyzing $LiBH_4-MgH_2$ has also been described, but unfortunately, the practical application of these systems are hampered by slow kinetics, limited reversibility, and the mechanism for dehydrogenation of $LiBH_4$ remains not fully understood.[19−21] Recently, cation substitution in borohydrides has been suggested, for example the synthesis of $LiK(BH_4)_2$, which unfortunately possesses the same high thermodynamic stability as the two compounds, $LiBH_4$ and KBH_4.[22] This calls for additional methods for modifying/improving materials properties and anion substitution has recently been suggested, e.g., by halide substitution in $LiBH_4$.[16,23,24]

Recent results indicate that solid LiCl dissolves in the structure of solid *h*-$LiBH_4$ by solid-state ion diffusion.[16] This is the first indication of a new and very promising method for modification of structure and properties of known borohydrides by anion substitution. This has prompted us to investigate the degree of chloride substitution as a function of temperature and the detailed structure and physical properties of lithium borohydride is studied here employing in situ synchrotron radiation powder X-ray diffraction (SR-PXD) and solid-state variable temperature (VT) MAS NMR spectroscopy. These techniques are complementary, i.e., SR-PXD probes long-range structural order whereas solid-state NMR provides information on the nearest coordination sphere of the studied nuclei and also on possible amorphous components in the investigated samples. Solid-state NMR spectra of powdered samples containing quadrupolar nuclei usually show significant line broadening caused by quadrupolar interactions, chemical shift anisotropy (CSA), and dipole−dipole couplings. Magic-angle spinning (MAS) of the sample can partly suppress the effects of these interactions, and combined with different decoupling techniques, high resolution solid-state NMR spectra may be obtained. In VT MAS NMR, the line width/shape of the spectrum contains information on the dynamics of the studied nucleus, its particular molecular fragment or molecule in the sample. For example, the ^{27}Al line width for lithium alanate ($LiAlH_4$) shows a decrease from 3.2 to 0.4 kHz when the sample changes from solid to the molten state at 180 °C.[25] Here, we present the results of a thorough and detailed combined SR-PXD and MAS NMR study on the structure and dynamics of the $LiBH_4-LiCl$ solid-solution performed as a function of temperature and time.

2. Experimental Section

Sample Preparation. A mixture of $LiBH_4$ and LiCl (1:1), 2.6 g in total, was ball milled using a sample to ball ratio of 1:35 by weight and a milling time of 120 min. The sample was thereafter sealed in an argon-filled quartz ampule and heated at 245 °C for 24 days. This sample is denoted s1 and is used to study the structure and degree of anion substitution. The Cl^- content in sample s1 varies in the different experiments due to a small segregation of Cl^- with time. The Cl^- content can be estimated from Rietveld refinement, the phase transition temperature, and time since preparation. Another sample, denoted s2, was prepared by ball milling $LiBH_4$ and LiCl (3:1) as described above and used to study the substitution process. Lithium borohydride, $LiBH_4$ (Aldrich, 95%), and lithium chloride, LiCl (Aldrich, 99.988%), were used as received. All sample handling was performed in an argon filled glovebox.

Synchrotron Radiation Powder X-ray Diffraction (SR-PXD). Synchrotron powder X-ray diffraction data were obtained at the Swiss-Norwegian Beamlines (SNBL) at the European Synchrotron Radiation Facility (ESRF), Grenoble, France. The premilled and preheated $LiBH_4-LiCl$ sample (s1, 1:1) was mounted under argon atmosphere in a 0.5 mm diameter quartz glass capillary, which was sealed with heat-resistant, water-free glue. The sample was subsequently heated and cooled three times continuously to 227 °C and cooled to −73 °C, at a rate of 2.5 °C/min, while SR-PXD data were collected in situ. The temperature was controlled by an Oxford Cryostream 700+. The data were collected using a MAR345 image plate detector at the BM01A line of SNBL. The data were measured at a sample

(11) Filinchuk, Y.; Chernyshov, D.; Černý, R. *J. Phys. Chem. C* **2008**, *112*, 10579–10584.
(12) Hartman, M. R.; Rush, J. J.; Udovic, T. J.; Bowman, R. C.; Hwang, S.-J. *J. Solid State Chem.* **2007**, *180*, 1298–1305.
(13) Dmitriev, V.; Filinchuk, Y.; Chernyshov, D.; Talyzin, A. V.; Dzwilewski, A.; Andersson, O.; Sundqvist, B.; Kurnosov, A. *Phys. Rev. B* **2008**, *77*, 174112.
(14) Miwa, K.; Ohba, N.; Towata, S.; Nakamori, Y.; Orimo, S. *Phys. Rev. B* **2004**, *69*, 245120.
(15) Smith, M. B.; Brass, G. E., Jr. *J. Chem. Eng. Data* **1963**, *8*, 342.
(16) Mosegaard, L.; Møller, B.; Jørgensen, J. E.; Filinchuk, Y.; Cerenius, Y.; Hanson, J. C.; Dimasi, E.; Besenbacher, F.; Jensen, T. R. *J. Phys. Chem. C* **2008**, *112*, 1299–1303.
(17) Vajo, J. J.; Skeith, S. L.; Mertens, F. *J. Phys. Chem. B* **2005**, *109*, 3719–3722.
(18) Bösenberg, U.; Doppiu, S.; Mosegaard, L.; Barkhordarian, G.; Eigen, N.; Borgschulte, A.; Jensen, T. R.; Cerenius, Y.; Gutfleisch, O.; Klassen, T.; Dornheim, M.; Bormann, R. *Acta Mater.* **2007**, *55*, 3951–3958.
(19) Yu, X. B.; Grant, D. M.; Walker, G. S. *Chem. Commun.* **2006**, *37*, 3906–3908.
(20) Mao, J. F.; Wu, Z.; Chen, T. J.; Weng, B. C.; Xu, N. X.; Huang, T. S.; Guo, Z. P.; Liu, H. K.; Grant, D. M.; Walker, G. S.; Yu, X. B. *J. Phys. Chem. C* **2007**, *111*, 12495–12498.
(21) Mosegaard, L.; Møller, B.; Jørgensen, J. E.; Bösenberg, U.; Dornheim, M.; Hanson, J. C.; Cerenius, Y.; Walker, G.; Jakobsen, H. J.; Besenbacher, F.; Jensen, T. R. *J. Alloys Compd.* **2007**, *446−447*, 301–305.
(22) Nickels, E. A.; Jones, M. O.; David, W. I. F.; Jonson, S. R.; Lowton, R. L.; Sommarva, M.; Edwards, P. P. *Angew. Chem., Int. Ed.* **2008**, *47*, 2817–2819.
(23) Mosegaard, L.; Møller, B.; Jørgensen, J. E.; Cerenius, Y.; Hanson, J. C.; Besenbacher, F.; Jakobsen, H. J; Jensen, T. R. Dehydrogenation of $LiBH_4$ Investigated using *in-situ* Synchrotron X-ray Diffraction and MAS NMR. Presented at MH2006 International Symposium on Metal-Hydrogen Systems, Lahaina, HI, October 1−6, **2006**.
(24) Maekawa, H.; Matsuo, M.; Takamura, H.; Ando, M.; Noda, Y.; Karahashi, T.; Orimo, S. *J. Am. Chem. Soc.* **2009**, *131*, 894–895.
(25) Wiench, J. W.; Balema, V. P.; Pecharsky, V. K.; Pruski, M. *J. Solid State Chem.* **2004**, *177*, 648–653.

to detector distance of 200 mm, using a selected wavelength of $\lambda = 0.652812$ Å. The detector parameters and the wavelength were calibrated with a standard sample of LaB_6 from NIST. The X-ray exposure time was 30 s, and the detector read out time was 53 s, which gives ~83 s per image and a total of 404 powder diffractograms were measured. The two-dimensional (2D) data were integrated using the Fit2D program.[26] Excellent counting statistics allowed us to define precisely the background line and to observe very weak diffraction peaks. Accurate integrated intensities were obtained due to a good powder average achieved by projecting the 3D scattering information on the 2D detector. Uncertainties of the integrated intensities were calculated at each 2θ-point by applying Poisson statistics to the intensity data, considering the geometry of the detector.[27] The calculated absorption coefficient is practically equal to zero, thus the absorption correction was not applied. Finally, the data were refined using the sequential refinement approach implemented in Fullprof.[28]

Another set of in situ SR-PXD data were collected at variable temperatures at beamline I711 in the research laboratory MAX-Lab, at the synchrotron facility MAX-II, Lund, Sweden, and at beamline X7B, National Synchrotron Light Source (NSLS), Brookhaven National Laboratory, using selected wavelengths of $\lambda = 1.1351$ and 0.92172 Å, respectively.[29] The data were collected on a MAR165 area charge-coupled device (CCD) detector or a MAR345 image plate system (MAX-Lab and NSLS, respectively). The sample cell was specially developed for studies of gas/solid reactions and allows high pressure and temperature to be applied.[30−32] The sample was placed in a sapphire tube mounted in a steel holder by vespel ferrules, and a chromel−alumel thermocouple was inserted into the sapphire tube and gave a feed back to the temperature controlled heating performed by a resistance heater wrapped around the sample. The gas system was repeatedly flushed with nitrogen and evacuated before a valve placed a few centimeters from the sample was opened. An X-ray exposure time of 30 or 60 s was used for data acquisition. A ball milled sample of $LiBH_4$ and LiCl (3:1) was heated from room temperature (RT) to 250 °C with a heating rate of 5 °C/min, and a sample of $LiBH_4$ was heated from RT to 600 °C with a heating rate of 3 °C/min. The frames were integrated using the Fit2D software,[26] and the observed powder patterns from both samples were readily indexed in order to explore the thermal expansion and the anion substitution process.

Structural Refinements. Rietveld refinements were performed using the Fullprof program and coordinates and atomic displacement factors from single-crystal diffraction studies of $LiBH_4$ and LiCl.[11,33] One overall temperature factor was refined for each type of atom in order to correct for the temperature changes. The data were split in a series each containing either diffraction from *o*- or *h*-$LiBH_4$ and the first patterns of each series (no. 1, 85, 206, 328 and no. 18, 129, 249, respectively) were refined with all linearly interpolated background points varied and the preliminarily determined zero shift fixed. The sequential refinement in Fullprof was used to refine the rest of the powder patterns in each series with pseudo-Voigt profile functions and all parameters,[34] including those structurally refined in a full matrix. Two different structural models were used for the orthorhombic phase of the substituted sample: (model 1) Chloride ions were constrained to the atomic position of boron in the BH_4^- ions in the structure of $LiBH_4$ and their total occupancy was constrained to one. (model 2) No substitution was considered and only refinement of pure nonreacted $LiBH_4$ and LiCl was considered. Model 1 was also used for the refinement of the data for the hexagonal phase. In general, Rietveld refinement of accurate powder X-ray diffraction data provides highly accurate unit cell parameters but less accurate compositional parameters based on refined occupancies. This is due to a strong correlation between occupation and thermal displacement parameters. The refinements for the data in Table 1 were performed by refining one pattern at each temperature as described above, and keeping the overall displacement factor fixed for the refinement of the pattern at the same temperature. Crystal data and structural refinement parameters are given in the Supporting Information.

Solid-State MAS NMR Spectroscopy. Solid-state ^1H, ^7Li, and ^{11}B magic-angle spinning (MAS) NMR spectra of $LiBH_4$ and chloride substituted samples $Li(BH_4)_{1-x}Cl_x$ were recorded at 399.8, 155.4, and 128.3 MHz, respectively, on a Varian INOVA-400 (9.4 T) spectrometer using a home-built variable temperature (VT) MAS probe for 5 mm o.d. Si_3N_4 rotors (110 μL sample volume) and a spinning speed $\nu_R = 5$ kHz.[35] The Si_3N_4 rotor was loaded with $LiBH_4$ or $Li(BH_4)_{1-x}Cl_x$ in an argon filled glovebox, and the rotors were closed using a Torlon end-cap equipped with two Viton O-rings. This ensured an airtight and inert environment for the sample, when outside the glovebox, for at least 30 days. The home-built variable temperature (VT) unit[36] was operated in the temperature range from ambient to about 130 °C, and the experiments were performed using very dry ordinary air with a dew point of −90 °C for controlling sample temperature and spinning speed. The temperature of the sample in the spinning rotor was calibrated by measurement of the chemical shift for the ^{207}Pb signal of $Pb(NO_3)_2$ under the exact identical spinning conditions and using a temperature coefficient of 0.758 ppm/°C.[36] A precision of ± 1 °C was obtained for the temperature measurement.

The ^1H MAS experiments employed an rf field strength of $\gamma B_1/2\pi = 62$ kHz, a pulse width of 2.0 μs, a relaxation delay of 4 s, and typically 32 scans. These conditions were found to give quantitative reliable intensities in the ^1H MAS NMR spectra. ^7Li MAS spectra were recorded using a rf field strength of $\gamma B_1/2\pi = 71$ kHz, a pulse width of 4.0 μs, a relaxation delay of 4 s, and typically 512 scans. An external sample of 1 M aqueous LiCl

(26) Fit2D program: Hammersley, A. P.; Svensson, S. O.; Hanfland, M.; Fitch, A. N.; Häusermann, D. *High Pressure Res.* **1996**, *14*, 235–248.
(27) Vogel, S.; Ehm, L.; Knorr, K.; Braun, G. *Adv. X-ray Anal.* **2002**, *45*, 31.
(28) Rodriguez-Carvajal, J. Fullprof; Fullprof Suite, LLB Sacley & LCSIM: Rennes, France, 2003.
(29) (a) Cerenius, Y.; Ståhl, K.; Svensson, L. A.; Ursby, T.; Oskarsson, Å.; Albertsson, J.; Lijas, A. *J. Synchrotron Rad.* **2000**, *7*, 203–208. (b) Hastings, J. B.; Suortii, P.; Thomsolin, P.; Kvick, A.; Koetzle, T. *Nucl. Instrum. Methods* **1983**, *208*, 55–58.
(30) Clausen, B. S.; Steffensen, G.; Fabius, B.; Villadsen, J.; Feidenhans'l, R.; Topsøe, H. *J. Catal.* **1991**, *132*, 524–535.
(31) Rodriguez, J. A.; Hanson, J. C.; Frenkel, A. I.; Kim, J. Y.; Perez, M. *J. Am. Chem. Soc.* **2002**, *124*, 346–354.
(32) Ravnsbæk, D.; Mosegaard, L.; Jørgensen, J. E.; Jensen, T. R. Proceedings of the 29th Risø International Symposium on Materials Science: Energy Materials−Advances in Characterization, Modelling and Application; Andersen, N. H., Eldrup, M., Hansen, N., Jensen, D. J., Nielsen, E. M., Nielsen, S. F., Sørensen, B. F., Pedersen, A. S., Vegge, T., West, S. S., Eds.; Risø National Laboratory for Sustainable Energy, Technical University of Denmark, **2008**, pp 349−356.
(33) Ott, H. *Phys. Z.* **1923**, *24*, 209–213.
(34) Hagemann, H.; Filinchuk, Y.; Chernyshov, D.; van Beek, W. *Phase Trans.* **2009**, *82*, 344–355.
(35) Jakobsen, H. J.; Daugaard, P.; Langer, V. *J. Magn. Reson.* **1988**, *76*, 162; U.S. patent 4739270.
(36) (a) Schönwandt, B. V; Jakobsen, H. J *J. Solid State Chem.* **1999**, *145*, 10–14. (b) Schönwandt, B. Design and Application of Instrumentation for Variable Temperature MAS NMR spectroscopy. M. Sc. Thesis, University of Aarhus, Aarhus, Denmark, **1998**.

Table 1. Unit Cell Parameters for Polymorphs of Lithium Borohydride, Lithium Chloride, and the Solid Solution $LiBH_4$−LiCl

	a/Å	b/Å	c/Å	V/Å^3	T/°C
o-$LiBH_4$[a]	7.141(5)	4.431(3)	6.748(4)	213.5(2)	−58
o-$Li(BH_4)_{0.91}Cl_{0.09}$ (cycle 1)[b]	7.143(1)	4.4032(8)	6.791(1)	213.65(7)	22
o-$Li(BH_4)_{0.71}Cl_{0.29}$ (cycle 2)[b]	7.009(1)	4.3266(9)	6.809(1)	206.53(7)	24
o-$Li(BH_4)_{0.70}Cl_{0.30}$ (cycle 3)[b]	7.001(1)	4.3236(9)	6.808(1)	206.10(7)	21
h-$LiBH_4$[a]	4.3228(10)	4.3228(10)	7.0368(10)	113.88(4)	262
h-$Li(BH_4)_{0.58}Cl_{0.42}$ (cycle 1)[b]	4. 2130(3)	4.2130(3)	6.7673(7)	104.025(9)	224
h-$Li(BH_4)_{0.58}Cl_{0.42}$ (cycle 2)[b]	4.2153(3)	4.2153(3)	6.7717(7)	104.205(9)	224
h-$Li(BH_4)_{0.58}Cl_{0.42}$ (cycle 3)[b]	4.2139(3)	4.2139(3)	6.7691(7)	104.096(9)	224
LiCl (cycle 1)[b]	5.1363(2)	5.1363(2)	5.1363()	135.508(9)	22
LiCl[c]	5.143(6)	5.143(6)	5.143(6)	136.03	25

[a] Reference 11. [b] This work. [c] Reference 33.

was used as ^{7}Li chemical shift reference. The ^{11}B MAS experiments employed a rf field strength of $\gamma B_1/2\pi = 60$ kHz, a pulse width of 5.0 μs, a relaxation delay of 4 s, and typically 1024 scans. An aqueous solution of 1 M H_3BO_3 was used as a secondary external ^{11}B chemical shift reference, with a ^{11}B chemical shift of $\delta = 19.6$ ppm relative to the standard primary ^{11}B reference sample of $(C_2H_5)_2O\cdot BF_3$. Simulations of the ^{7}Li and ^{11}B MAS NMR spectra were performed on a SUN Ultra-5 workstation using the STARS solid-state NMR software package developed earlier for analysis and least-squares fitting of MAS NMR spectra.[37]

Physical Measurements. Differential scanning calorimetry (DSC) and thermogravimetric analysis (TGA) were performed simultaneously using a Netzch STA449C Jupiter instrument (22−350 °C, heating and cooling rates of 2.5 and 5.0 °C/min, respectively) and aluminum oxide crucibles with lids were used as sample holders. Samples of $LiBH_4$ and $Li(BH_4)_{1-x}Cl_x$ (s1) were used to determine the physical properties such as phase transition temperature and melting point. Three heating and cooling cycles were performed to compare this experiment with the in situ SR-PXD experiment.

A PCTPro2000 apparatus[38] equipped with a home-built sample holder was used to perform temperature programmed desorption (TPD) measurements on $LiBH_4$ and $Li(BH_4)_{1-x}Cl_x$ (s1). The samples were heated to 550 °C with a constant heating rate of 0.5 °C/min.

3. Results and Discussion

Synthesis and Chloride Substitution Process. In situ SR-PXD experiments with $LiBH_4$ and with a mixture of ball milled $LiBH_4$ and LiCl (3:1 molar ratio, s2) have been performed in order to study the anion-substitution process. Figure 1 shows the unit cell volume as a function of temperature for the two samples. Both samples show similar thermal expansion in the temperature range RT to 115 °C (in the orthorhombic phase). Interestingly, after the phase transition to *h*-$LiBH_4$, the unit cell volume of the mixed sample (s2) decreases, whereas that of $LiBH_4$ shows the positive thermal expansion.[11] The decrease in the volume for the lithium chloride containing sample (s2) is attributed to the substitution of the larger BH_4^- complex ion in the structure of $LiBH_4$ with the smaller Cl^- ion. It is noteworthy that the substitution is a relatively fast process (heating rate 5 °C/min) at relatively low temperatures (106−200 °C). Second, the substitution process clearly shows a preference for the hexagonal phase as compared to the orthorhombic phase, which might be due to the higher dynamic in the hexagonal phase as compared to the orthorhombic phase.

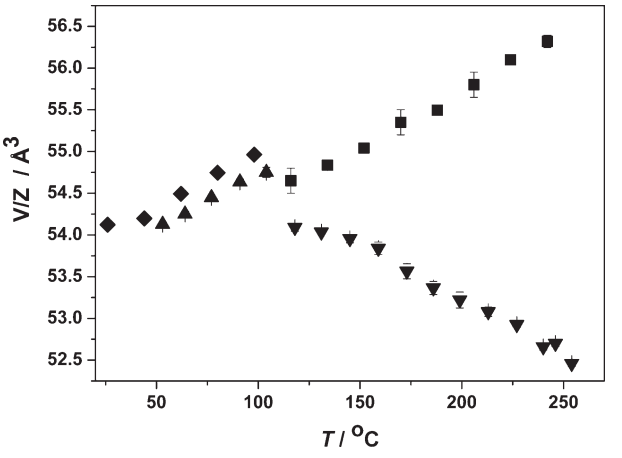

Figure 1. Unit cell volume per formula unit of the structure of $LiBH_4$ and $Li(BH_4)_{1-x}Cl_x$ found in $LiBH_4$−LiCl (3:1 molar ratio, s2) in the temperature range 20 and 250 °C with heating rates 3 and 5 °C/min, respectively. Symbols: ♦ *o*-$LiBH_4$, ■ *h*-$LiBH_4$, ▲ *o*-$Li(BH_4)_{1-x}Cl_x$, ▼ *h*-$Li(BH_4)_{1-x}Cl_x$.

Structure and Composition of $Li(BH_4)_{1-x}Cl_x$ ($0.09 \leq x \leq 0.42$). In order to reach equilibrium conditions for the substitution process, a sample of $LiBH_4$−LiCl (1:1, s1) was heated under inert conditions for a prolonged period of time (245 °C for 24 days). This sample (s1) was then equilibrated for 13 months at RT and then examined by high resolution SR-PXD from RT to 227 °C. The amount of Cl^- in the initial sample (equilibrated for 13 months) was found from Rietveld refinement to be $x = 0.09$. A series of three continuous heating and cooling cycles were performed for $Li(BH_4)_{0.91}Cl_{0.09}$ (s1), and all data were refined by the Rietveld method. Structural model 1 has been used where Cl^- substitutes for BH_4^- in the structure of $LiBH_4$ and the center of the BH_4^- units and the Cl^- atoms are constrained to the same set of x, y, z coordinates and their occupancies sum to one. Furthermore, for the first pattern, a refinement has been performed with model 2, which assumes no substitution of Cl^- into the structure and only a mixture of pure $LiBH_4$ and LiCl. The obtained Bragg R-factors for the first

(37) Jakobsen, H. J.; Skibsted, J.; Bildsoe, H.; Nielsen, N. C. *J. Magn. Reson.* **1989**, *85*, 173. See also: Varian Manual, STARS (SpecTrum Analysis for Rotating Solids), Publication No. 87-195233-00, 1996, Rev. A0296.

(38) (a) www1.eere.energy.gov/HYDROGENANDFUELCELLS/PDFS/BESTPRACTICES_H2_STORAGE_MATERIALS.PDF (accesssed November 10, 2009). (b) http://www.setaram.com/PCTPro-2000.htm (accesssed November 10, 2009).

pattern with models 1 and 2 are 3.69, 0.812 and 21.0, 1.44, respectively, which clearly show a preference for model 1. The unit cell parameter of LiCl is found to be a = 5.13635(2) Å, which agrees well with the published data, a = 5.143(6) Å.[33] Therefore, it is concluded that the data give no indication of anion substitution in the structure of LiCl. In contrast, the volume of the new phase $Li(BH_4)_{1-x}Cl_x$ ($0.09 \leq x \leq 0.42$) is found to be significantly smaller by up to ~3.2% for the orthorhombic phase (third cycle) and 8.7% for the hexagonal phase (first cycle) than previously published data for *o*- and *h*-$LiBH_4$; see Table 1. This is in good agreement with the fact that the ionic radius of Cl^- (r = 1.81 Å) is smaller than BH_4^- (r = 2.05 Å).[39] Interestingly, it is observed that upon Cl^- substitution for BH_4^- the cell parameters for the orthorhombic phase change anisotropically, with a and b decreasing and c increasing, whereas the hexagonal phase contracts isotropically. Furthermore, it is concluded that a maximum of 38.0 wt % (30 mol %) Cl^- can be substituted into the structure for the orthorhombic phase of $LiBH_4$ (cycle 3), resulting in the composition *o*-$Li(BH_4)_{0.70}Cl_{0.30}$. This demonstrates that Cl^- ions can substitute for BH_4^- ions in *h*-$LiBH_4$ and that the obtained solid solution can be quenched to RT where the *o*-$Li(BH_4)_{0.70}Cl_{0.30}$ phase is obtained.

It is particularly noteworthy that the refinement of the hexagonal phase (cycle 1) at T = 224 °C shows that a higher quantity of Cl^- ions can be substituted into the high temperature phase resulting in a Cl-rich composition $Li(BH_4)_{0.58}Cl_{0.42}$, which corresponds to 48.9 wt % (42 mol %) Cl^-. For the sample obtained at 224 °C, the refinement converged at $R_{Bragg}(Li(BH_4)_{0.58}Cl_{0.42})$ = 10.8% and $R_{Bragg}(LiCl)$ = 0.7%. The determined unit cell parameters are summarized in Table 1. It is clearly seen that the unit cell parameters are smaller compared to pure $LiBH_4$, which further confirm the higher substitution rate. The calculated intensity and difference plots for the refinements of the orthorhombic and hexagonal phase can be found in the Supporting Information.

The above-mentioned structural results indicate that the unit cell volume can be used as an indirect measure of the composition or degree of lithium chloride substitution in lithium borohydride. A sample of anion substituted lithium borohydride, $Li(BH_4)_{0.91}Cl_{0.09}$, was cycled three times in the temperature interval −73 to 227 °C (2.5 °C/min); see Figure 2. Initially (Figure 2a), *o*-$Li(BH_4)_{0.91}Cl_{0.09}$ shows thermal expansion up to the *o*- to *h*-$Li(BH_4)_{1-x}Cl_x$ phase transition; hereafter, *h*-$Li(BH_4)_{1-x}Cl_x$ clearly show decreasing unit cell volume with increasing temperature due to significant dissolution of LiCl. The composition of *h*-$Li(BH_4)_{1-x}Cl_x$ is in the range $0.21 \leq x \leq 0.42$ for the first heating and reaches a maximum of $Li(BH_4)_{0.58}Cl_{0.42}$ at the end of the cycle. It is clearly seen that the volume of $Li(BH_4)_{0.91}Cl_{0.09}$ before the first cycle is much higher than after, demonstrating the substitution

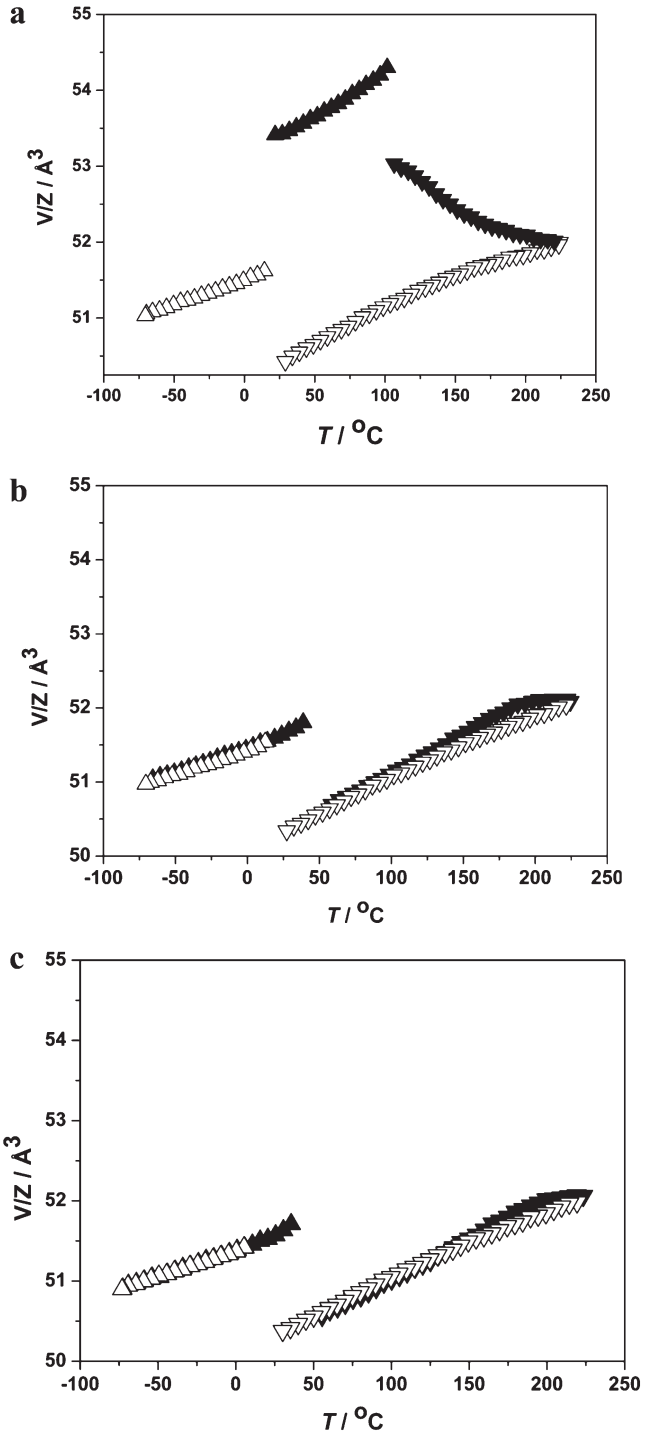

Figure 2. Unit cell volume per formula unit of the $Li(BH_4)_{1-x}Cl_x$ ($0.09 \leq x \leq 0.42$) structures for the (a) first, (b) second, and (c) third heating and cooling cycles. Symbols: ▲ *o*-$Li(BH_4)_{1-x}Cl_x$ (heating), ▼ *h*-$Li(BH_4)_{1-x}Cl_x$ (heating), △ *o*-$Li(BH_4)_{1-x}Cl_x$ (cooling), ▽ *h*-$Li(BH_4)_{1-x}Cl_x$ (cooling).

of Cl^- during the first heating cycle. In the second and third heating and cooling cycles, only minor compositional changes are observed. This is illustrated in Figure 2b and c by thermal expansion of $Li(BH_4)_{1-x}Cl_x$ ($0.28 \leq x \leq 0.42$). The unit cell volumes as a function of temperature during the second and third cycles are similar indicating that a complete substitution at the selected conditions has occurred. The curve appears to flatten around 227 °C, but the substitution of lithium chloride

(39) *CRC Handbook of Chemistry and Physics*, 88th ed.; Lide, D. R., Ed.; CRC: Boca Raton, 2007, pp 12−27.

Table 2. Composition (x) at a Given Temperature and Phase Transition Temperature for $LiBH_4$−LiCl (s1) $Li(BH_4)_{1-x}Cl_x$ during Three Cycles of Heating and Cooling ($\Delta T/\Delta t = \pm 2.5$ °C)

heating/cooling cycle		composition		phase transition		hysteresis
no.	x_{Cl}(23 °C)	x_{Cl}(224 °C)	x_{Cl}(−70 °C)	$T(o \rightarrow h)$ (°C)	$T(h \rightarrow o)$ (°C)	ΔT (°C)
1	0.09	0.42	0.27	102	24	78
2	0.29	0.42	0.28	44	22	21
3	0.30	0.42	0.28	41	20	20

Table 3. Linear Thermal Expansion Coefficients of $LiBH_4$ (Data Shown in Figure 1) and $Li(BH_4)_{1-x}Cl_x$ $0.29 \leq x \leq 0.42$ (second cycle, Figure 2b)

sample	range T/°C	a-axis $\alpha_a/10^{-5}$ K^{-1}	b-axis $\alpha_c/10^{-6}$ K^{-1}	c-axis $\alpha_c/10^{-5}$ K^{-1}	volumen $\alpha_{vol}/10^{-5}$ K^{-1}
o-$LiBH_4$	25−115	6.92	7.89	16.10	23.03
o-$Li(BH_4)_{0.71}Cl_{0.29}$	−70−40	2.86	2.62	8.95	13.33
h-$LiBH_4$	116−255	7.68	7.68	9.77	25.46
h-$Li(BH_4)_{0.58}Cl_{0.42}$	40−216	7.20	7.20	5.98	19.95

may increase further if the temperature is raised or held constant at 227 °C for a prolonged period of time.

These experiments (Figure 2) reveal that the dissolution of lithium chloride in h-$LiBH_4$ is a relatively fast process mediated by solid-state ion diffusion. On the other hand, segregation of lithium chloride from solid $Li(BH_4)_{1-x}Cl_x$ ($0.28 \leq x \leq 0.42$) is a relatively slow process at RT. The substitution and precipitation rates at low and high temperatures naturally correlate with the diffusion speed as a function of temperature. Note, that sample s1 was initially equilibrated for 24 days at 245 °C, but after 13 months, the chloride content has decreased to $Li(BH_4)_{0.91}Cl_{0.09}$. A small broadening of the diffraction peaks from o- and h-$Li(BH_4)_{1-x}Cl_x$ was observed after the different heating and cooling cycles, possibly due to a larger concentration gradient of Cl^- in the freshly heated samples, compared to the initial sample.

In the first cycle, the phase transition temperature of o- to h-$Li(BH_4)_{1-x}Cl_x$ is observed to be $T = 106$ °C, which is similar to $LiBH_4$ at 108 °C.[11] Interestingly, the phase transition temperature clearly decreases during the cycling and in the third cycle it is already observed at 41 and 20 °C for heating and cooling, respectively. A clear correlation is seen between the amount of Cl^- substituted in the structure and the temperature for the phase transition, Table 2. This clearly shows that the anion substitution stabilizes the hexagonal phase in agreement with earlier work.[40] The stabilization of the hexagonal phase by substitution of Cl^- may facilitate the rehydrogenation of the system.[41]

Interestingly, weak diffraction from an intermediate phase is observed at 59 °C during the first cooling of the sample before the phase transition from h- to o-$Li(BH_4)_{1-x}Cl_x$ (Figure 3). The intermediate phase coexists with the hexagonal phase and disappears when the orthorhombic phase appears. This intermediate phase is again observed in the second and third heating/cooling cycles and is therefore related to the Cl^- content in the sample; it exists during heating in the temperature range 39−74 °C.

The linear thermal expansion coefficient is calculated using the equation $\alpha_L = L_0^{-1} \cdot (L_{final} - L_{initial})/(T_{final} - T_{initial})$,

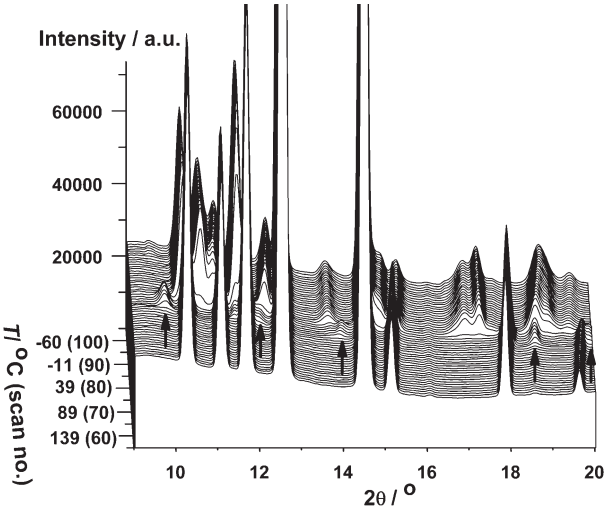

Figure 3. In situ SR-PXD data measured during the first cooling (Figure 2a) shows an intermediate (arrows) appearing at 59 °C (cooling rate 2.5 °C) prior to the transition from o- to h-$Li(BH_4)_{1-x}Cl_x$ ($0.28 \leq x \leq 0.42$) ($\lambda = 0.652812$ Å).

where L denotes a unit cell axis or volume and L_0 is the extrapolated value at 0 °C. The results for the anion-substituted $LiBH_4$ are summarized in Table 3 and compared to those for pure $LiBH_4$. In general, $LiBH_4$ has higher thermal expansion coefficients as compared to the substituted sample. Furthermore, it is quite clear that the thermal expansion coefficient for o-$LiBH_4$ is about twice as large as the coefficient for o-$Li(BH_4)_{0.71}Cl_{0.29}$. However, for h-$LiBH_4$, the coefficient for the volume expansion is only about 20% larger as compared to that for h-$Li(BH_4)_{0.58}Cl_{0.42}$. The expansion of the c-axis for h-$LiBH_4$ is observed to be larger compared to the expansion of the c-axes for the substituted sample, which is in contrast to the expansion of the a-axes of the two samples, which are similar.

Solid-State MAS NMR Spectroscopy of $LiBH_4$ and $Li(BH_4)_{1-x}Cl_x$. The phase transition of o-$LiBH_4$ to h-$LiBH_4$ has been investigated by ^{7}Li, ^{11}B, and ^{1}H VT MAS NMR spectroscopies. These are performed for both $LiBH_4$ and the anion-substituted $Li(BH_4)_{0.86}Cl_{0.14}$ solid solution (sample s1, 6 months after preparation, when x is estimated to be 0.14 from the phase transformation temperature) in order to gain information about the

(40) Matsuo, M.; Takamura, H.; Maekawa, H.; Li, H. W.; Orimo, S. I. *Appl. Phys. Lett.* **2009**, *94*, 084103.
(41) Pinkerton, F. E; Meyer, M. S. *J. Alloys Compd.* **2008**, *464*, L1–L4.

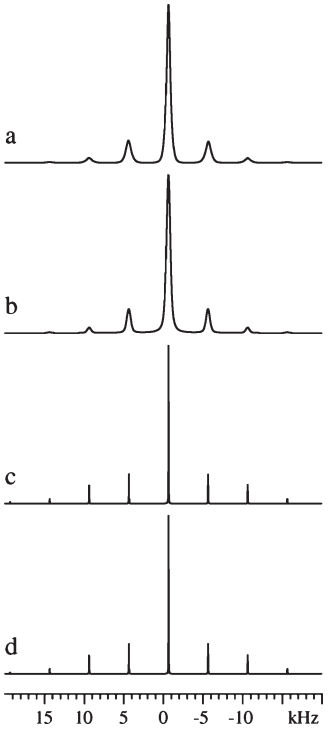

Figure 4. (a) Observed ^{7}Li MAS NMR spectrum of *o*-$LiBH_4$ at RT. (b) Optimized fitted and simulated spectrum of the experimental data shown in part a. (c) Observed ^{7}Li MAS NMR spectrum of $LiBH_4$ at 121 °C. (d) Optimized fitted and simulated spectrum of the spectrum shown in part c. The parameters from the least-squares fit to the observed data are given in Table 4.

dynamic and physical changes of the structures during the phase transition.

^{7}Li MAS NMR on $LiBH_4$. The observation of only a single ^{7}Li resonance for $LiBH_4$ as well as for $Li(BH_4)_{0.86}Cl_{0.14}$ is in accordance with the crystal structural model for *o*- and *h*-$LiBH_4$, which is described by one Li position in the asymmetric unit. This also demonstrates that the structure of $Li(BH_4)_{0.86}Cl_{0.14}$ is similar to $LiBH_4$ as shown by Rietveld refinement in this study. On the other hand, the ^{7}Li MAS NMR spectra for the *o*- and *h*-$LiBH_4$ appear quite different as illustrated in Figure 4. The spectrum acquired at the ambient temperature of 24 °C (*o*-$LiBH_4$) using a spinning frequency $\nu_r = 5000$ Hz is shown in Figure 4a and displays a line width fwhm (full width at half maximum) for the central transition of about 550 Hz. This line width is dramatically reduced to only 26 Hz observed in the spectrum (Figure 4c) acquired at a higher temperature of 123 °C for *h*-$LiBH_4$ just above the phase transition. The experimental ^{7}Li MAS NMR spectra in Figure 4a and c have been analyzed in terms of the quadrupole coupling constant (C_Q) and the asymmetry parameter (η_Q) for this quadrupolar nucleus ($I = 3/2$). Optimized fitting of simulated to the experimental line shapes and intensities for the central and satellite transitions yields the optimized parameters listed in Table 4 and the corresponding simulations of the spectra are illustrated in Figures 4b and d. For the spectrum of *o*-$LiBH_4$ ($T = 24$ °C), $C_Q = 17.9$ kHz and $\eta_Q = 0.98$ are obtained where the uncertainty for η_Q is high, since fairly good fits to the experimental spectrum can be obtained for any η_Q value in the range $0.30 \leq \eta_Q \leq 1$. For *h*-$LiBH_4$ ($T = 123$ °C), the optimized fitting of the spectrum yields $C_Q = 36.4$ kHz and $\eta_Q = 0.19$ with a somewhat better precision as compared to the data for the *o*-$LiBH_4$. Moreover, for *h*-$LiBH_4$, a value for $C_Q = 32$ kHz (but not for η_Q) has recently been evaluated from static (nonspinning) ^{7}Li NMR spectra,[42] which is in quite good agreement with the data presented here determined from MAS NMR. It was not possible to extract values for C_Q and η_Q from the extremely broadened static ^{7}Li NMR spectra measured for *o*-$LiBH_4$ in the previous studies[42] in contrast to the present MAS NMR study.

Table 4. Solid-State NMR Parameters for Pure $LiBH_4$ and $Li(BH_4)_{1-x}Cl_x$[a]

	C_Q (kHz)	η_Q (−)	δ_{iso} (ppm)	T (°C)
		^{7}Li		
o-$LiBH_4$	17.9	0.28−0.98	−0.91	24
o-$LiBH_4$	17.4	0.98	−0.97	71
o-$LiBH_4$	16.3	0.76	−0.96	88
o-$LiBH_4$	15.9	0.67	−0.89	105
o-$LiBH_4$	14.9	0.63	−0.84	113
h-$LiBH_4$	36.4	0.19	−0.97	123
o-$Li(BH_4)_{0.86}Cl_{0.14}$	19.7	0.97	−0.81	24
o-$Li(BH_4)_{0.86}Cl_{0.14}$	18.1	0.88	−0.91	72
h-$Li(BH_4)_{1-x}Cl_x$[b]	27.1	0.39	−0.91	120
		^{11}B		
o-$LiBH_4$	99	0.91	−41.0	25

[a] The error limits for the ^{7}Li NMR parameters are: C_Q (±0.5 kHz), η_Q (±0.3), and δ_{iso} (±0.2 ppm). For the ^{11}B NMR parameters, the error limits are the following: C_Q (±3 kHz), η_Q (±0.2), δ_{iso} (±0.5 ppm), $\delta_\sigma = 30 \pm 3$ ppm, and $\eta_\sigma = 0.91 \pm 0.2$. [b] $0.14 \leq x \leq 0.42$.

The ^{7}Li MAS NMR spectra recorded for *o*-$LiBH_4$ (24 °C ≤ T ≤ ∼119 °C) in a VT experiment starting from ambient and approaching the phase transition temperature (∼119 °C) exhibit an interesting feature for the fwhm of the central transition, as shown in Figure 5. In the temperature range 24−100 °C, the fwhm is fairly constant with a slight decrease from 550 to 498 Hz. However, at about 100 °C, the fwhm begins to increase from 498 Hz to about 800 Hz at a temperature of 119 °C where the phase transition to *h*-$LiBH_4$ starts to occur. The fwhm abruptly decreases to about 60 Hz at 121 °C where the phase transition appears to be completed. In addition, this figure also shows that by approaching the phase transition starting from the *h*-$LiBH_4$ phase (i.e., by a decrease in temperature), the phase transition temperature returning into the *o*-$LiBH_4$ phase starts at about 111 °C, which is about 10 °C lower than for the *o*- to *h*-$LiBH_4$ phase transition. This hysteresis of about 10 °C was also recently observed in a study of the temperature dependence of the electrical conductivity for $LiBH_4$ and is a commonly encountered feature observed in solid-state MAS NMR studies of structural phase transitions.[42,44,45] The

(42) Matsuo, M.; Nakamori, Y.; Orimo, S. I.; Maekawa, H.; Takamura, H. *Appl. Phys. Lett.* **2007**, *91*, 224103.
(43) Giavani, T.; Johannsen, K.; Jacobsen, C. J. H.; Blom, N.; Bildsøe, H.; Skibsted, J.; Jakobsen, H. J. *Solid State Nucl. Magn. Reson.* **2003**, *24*, 218–235.
(44) Bjornholm, T.; Jakobsen, H. J. *J. Magn. Reson.* **1989**, *84*, 204.
(45) Giavani, T.; Bildsøe, H.; Skibsted, J.; Jakobsen, H. J. *J. Phys. Chem B* **2002**, *106*, 3026–3032.

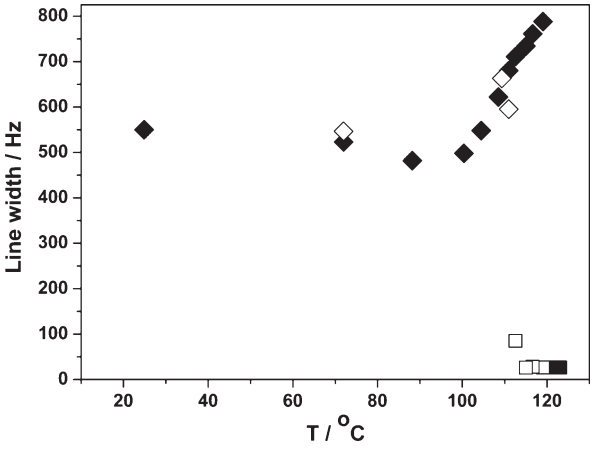

Figure 5. Full width at half maximum (fwhm) for the ^{7}Li central transition shown as a function of the temperature. Data were measured during heating and cooling in the temperature range 24−123 °C. Symbols: ♦ *o*-$LiBH_4$ (heating), ■ *h*-$LiBH_4$ (heating), ◊ *o*-$LiBH_4$ (cooling), □ *h*-$LiBH_4$ (cooling).

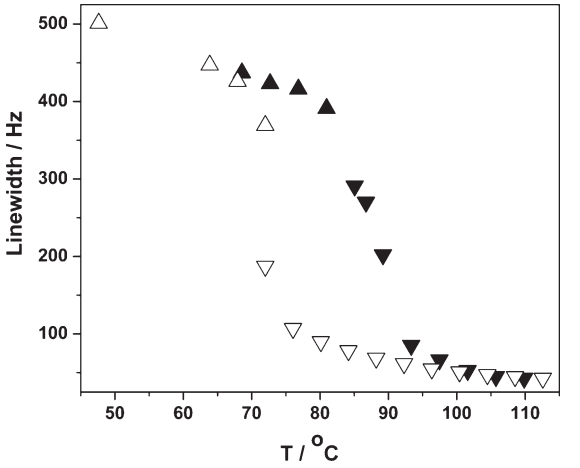

Figure 6. Full width at half maximum (fwhm) for the ^{7}Li central transition shown as a function of the temperature. Data were measured during heating and cooling of $Li(BH_4)_{1-x}Cl_x$ (s1, after 6 month) in the temperature range 24−115 °C. Symbols: ▲ *o*-$Li(BH_4)_{1-x}Cl_x$ (heating), ▼ *h*-$Li(BH_4)_{1-x}Cl_x$ (heating), △ *o*-$Li(BH_4)_{1-x}Cl_x$ (cooling), ▽ *h*-$Li(BH_4)_{1-x}Cl_x$ (cooling).

hysteresis effect may be due sluggishness of phase transition in the solid state. From the VT behavior of the fwhm for the central transition when approaching the phase transition by an increase in temperature, it is noteworthy that the $1/T_2(^7Li)$ relaxation rate (determined from the fwhm) becomes increasingly effective (i.e., T_2 decreases) due to the increase in librations and mobility within the $LiBH_4$ structure at temperatures initiating the phase transition. This contrasts the temperature dependence of the spin−lattice relaxation $T_1(^7Li)$ for $LiBH_4$ which increases in the corresponding temperature region as recently determined.[42] Finally, we point out that analysis of four additional spectra acquired in the temperature range 70−112 °C show a continuous minor decrease in the magnitudes for C_Q from 17.4 to 14.9 kHz accompanied by a similar decrease in η_Q from 0.98 to 0.63 (Table 4).

^{7}Li MAS NMR on $Li(BH_4)_{0.86}Cl_{0.14}$. The ^{7}Li MAS NMR spectra of the orthorhombic and hexagonal phases for the $Li(BH_4)_{0.86}Cl_{0.14}$ sample (See Supporting Information) exhibit very similar features to those shown for the $LiBH_4$ sample in Figure 5. The main difference between the spectra of the two different samples is that the temperatures for the hysteresis curve in Figure 6 for the orthorhombic to hexagonal and hexagonal to orthorhombic phase transitions in $Li(BH_4)_{0.86}Cl_{0.14}$ are significantly lower compared to the phase transitions in $LiBH_4$. Spectral analysis by optimized fitting to the experimental spectra gives similar parameters (C_Q = 19.7 kHz and η_Q = 0.97) for the orthorhombic solid solution (T = 24 °C) as observed for *o*-$LiBH_4$ (Table 4).

For the hexagonal solid solution, which is obtained from the *o*- to *h*- $Li(BH_4)_{0.86}Cl_{0.14}$ phase transition starting at about 81 °C and completed at about 100 °C, the ^{7}Li quadrupole coupling parameters are C_Q = 27.1 kHz and η_Q = 0.39 as determined from a spectrum acquired at 120 °C. The C_Q and η_Q values are also fairly similar to those obtained for $LiBH_4$ in its hexagonal phase. The fwhm values of the central transition in the ^{7}Li MAS NMR spectra for $Li(BH_4)_{0.86}Cl_{0.14}$ as a function of temperature are illustrated in Figure 6 and show a continuous decrease in the fwhm from about 490 to 380 Hz across the temperature range 24−81 °C for the orthorhombic phase followed by an abrupt decrease to 45 Hz at about 100 °C following the complete phase transition to *h*-$Li(BH_4)_{0.86}Cl_{0.14}$. The phase transition temperature corresponds quite well with that observed from the in situ SR-PXD data (41−102 °C, depending on the amount of Cl^-). The hysteresis for the solid solution amounts to about 15 °C, which is higher as compared to the hysteresis for *h*- to *o*-$LiBH_4$, but it is in good agreement with the in situ SR-PXD data. The fwhm values observed in the VT MAS NMR experiments for the substituted and pure $LiBH_4$ (Figure 5 and 6) display similar features and hysteresis curves, except that the increase in fwhm just prior to the phase transition for $LiBH_4$ (Figure 5) is not observed for $Li(BH_4)_{0.86}Cl_{0.14}$ (Figure 6). Thus, the abrupt change in dynamics starting at 100 °C, which initiates the phase transition for pure $LiBH_4$, does not take place for the $Li(BH_4)_{0.86}Cl_{0.14}$ solid solution. However, most importantly a decrease in the average temperature for the overall phase transition hysteresis curve of about 35 °C relative to that for pure $LiBH_4$ is observed. At this point we note that earlier in situ SR-PXD experiments also show a decrease in temperature for the orthorhombic to hexagonal phase transition for $Li(BH_4)_{0.86}Cl_{0.14}$ compared to that for pure $LiBH_4$.[40] In conclusion, our present NMR observations clearly indicate a stabilization of the hexagonal phase when chloride ions are incorporated into the structure of $LiBH_4$.

^{11}B Solid-State MAS NMR on $LiBH_4$. Experimental and simulated ^{11}B MAS NMR spectra are shown in Figure 7. Only a single resonance is observed for $LiBH_4$ in its ^{11}B MAS NMR spectrum, which is in accordance with the crystal structural model for $LiBH_4$, described by one boron position in the asymmetric unit.

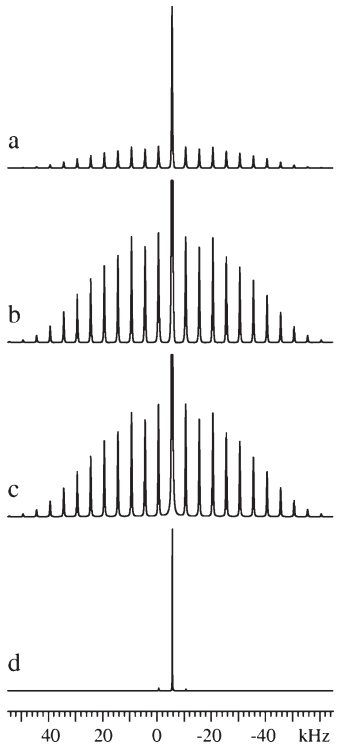

Figure 7. (a) Observed ^{11}B MAS NMR spectrum of *o*-$LiBH_4$ at RT. (b) Spectrum as in part a but the vertical scale is increased by a factor of 5. (c) Simulated spectrum following optimized fitting of the spectrum in part b (see text). (d) Observed ^{11}B MAS NMR spectrum of *h*-$LiBH_4$ at 120 °C. The parameters from the least-squares fit to the experimental spectra are given in Table 4.

The ^{11}B MAS NMR spectra of the *o*-$LiBH_4$ and *h*-$LiBH_4$ phases for $LiBH_4$ are widely different, as illustrated by the spectra shown in Figure 7. The spectrum acquired at RT, i.e., (below the phase transition) using a spinning frequency ν_r = 5000 Hz, is shown in Figure 7a and displays a line width fwhm for the central transition of about 360 Hz. This line width is dramatically reduced (60 Hz) in the ^{11}B MAS NMR spectrum (Figure 7d) acquired at a temperature of 120 °C (i.e., just above the phase transition). The experimental ^{11}B MAS NMR spectrum in Figure 7b, which represents an increase in the vertical scale expansion by a factor of 5 for the spectrum in 7a, has been analyzed in terms of the quadrupole coupling constant (C_Q) and asymmetry parameter (η_Q) for this quadrupolar nucleus (I = 3/2). Optimized fitting of simulated to the experimental line shapes and intensities of the central and satellite transitions yields the optimized parameters listed in Table 4, and the corresponding simulation for the experimental spectrum is illustrated in Figure 7c. To achieve the excellent fit (Figure 7c) of the spinning sideband intensities for the satellite transitions to that for the experimental spectrum requires a simultaneous optimization of both the ^{11}B C_Q, η_Q parameters, and ^{11}B chemical shift anisotropy (CSA) parameters (δ_σ, η_σ, δ_{iso}). Although the CSA appears to be quite small (δ_σ = 30 ppm, η_σ = 0.91), it is on the order of the values observed for other symmetrical ions, e.g., NR_4^+ published from earlier work on ^{14}N MAS NMR.[43] From the spectrum of the *o*-$LiBH_4$ phase, the quadrupolar coupling parameters C_Q = 99 kHz and η_Q = 0.91 are obtained. In the temperature range 70 to 116 °C, a reduction of the C_Q values is observed and a total collapse of the spectrum to a narrow single line (fwhm = 60 Hz) is observed at 116 °C caused by the phase transition.

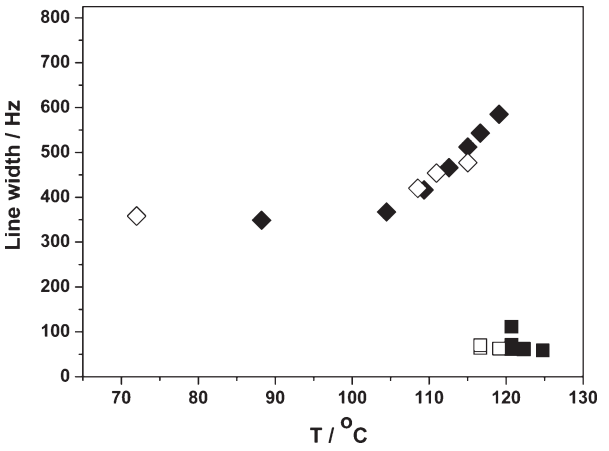

Figure 8. Full width at half maximum (fwhm) for the ^{11}B central transition shown as a function of the temperature. Data were measured during heating and cooling of pure $LiBH_4$ in the temperature range 24−123 °C. Symbols: ♦ *o*-$LiBH_4$ (heating), ■ *h*-$LiBH_4$ (heating), ◊ *o*-$LiBH_4$ (cooling), □ *h*-$LiBH_4$ (cooling).

The ^{11}B MAS NMR spectra for the VT experiment show the same complex behavior for the fwhm of the central transition for $LiBH_4$ as is observed for the ^{7}Li spectra when approaching the phase transition, as shown in Figure 8. In the temperature range 67 to 100 °C, the fwhm is fairly constant (375 Hz). However, at about 100 °C, the fwhm begins to increase from 357 Hz to about 600 Hz, until it suddenly drops to 70 Hz at a temperature of 117 °C where the transition to the *h*-$LiBH_4$ phase starts and appears to be completed at 120 °C. During cooling and approaching the phase transition from the *h*-$LiBH_4$ phase (i.e., by a decrease in temperature), the temperature for return into the *o*-$LiBH_4$ phase is observed at 112 °C, which is 5 °C lower than that for the *o*- to *h*-$LiBH_4$ phase transition. This hysteresis effect is similar to the one observed from the ^{7}Li MAS NMR experiments, although it is observed to be slightly lower in ^{11}B MAS NMR.

^{1}H Solid-State MAS NMR on $LiBH_4$. The proton spectra only showed a single relatively broad (fwhm = 2450 Hz) resonance in ^{1}H MAS NMR for a spinning frequency of 5 kHz. The line widths as a function of temperature from the ^{1}H MAS NMR are displayed in Figure 9. The fwhm follow more or less the same tendency as observed for the ^{7}Li and ^{11}B experiments for pure $LiBH_4$. First, it is constant at 2440 Hz from RT to approximately 100 °C, and then, it increases to 2720 Hz just before the phase transition at 116 °C, and finally, it decreases to the same value of about 2450 Hz as observed below the temperature of 100 °C. These ^{1}H MAS NMR results differ from the ^{7}Li and ^{11}B MAS NMR observation for pure $LiBH_4$ by having the same fwhm before and after the *o*- to *h*-$LiBH_4$ phase transition.

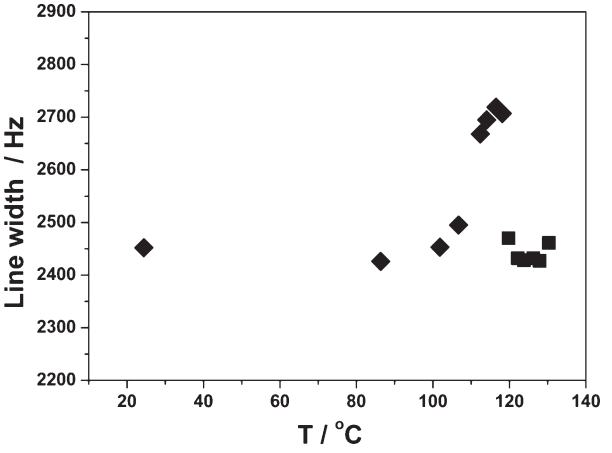

Figure 9. Full width at half maximum (fwhm) for the ^{1}H isotropic resonance shown as a function of the temperature. Data are measured during heating and cooling of pure $LiBH_4$ in the temperature range 24−123 °C. Symbols: ♦ *o*-$LiBH_4$ (heating), ■ *h*-$LiBH_4$ (heating).

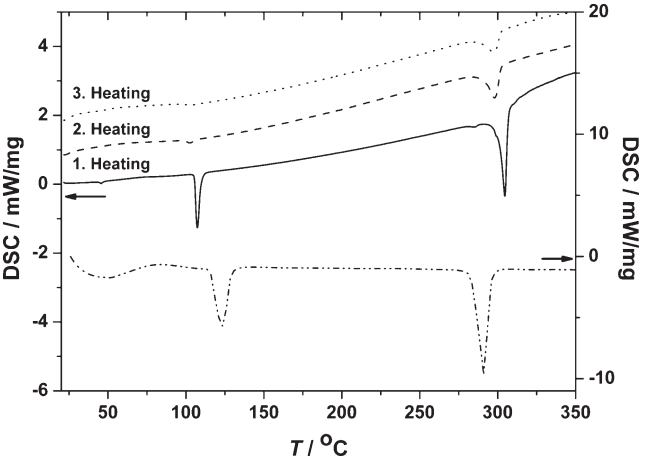

Figure 10. Differential scanning calorimetry measurement of $LiBH_4$ and $Li(BH_4)_{1-x}Cl_x$, (s1, x = 0.09 at the start of the experiment). Data measured from 22 to ca. 350 °C with a heating rate of 2.5 °C/min. Three heating cycles are shown for the substituted sample. The second and third heating is offset by 0.8 and 1.8, respectively. Symbols: $LiBH_4$ (dash dot dot); $Li(BH_4)_{1-x}Cl_x$, first (solid line), second (broken lines), and third (dots) heatings.

Although this behavior of the ^{1}H fwhm may seem somewhat puzzling,[46,47] it shows that a spinning frequency of ν_r = 5 kHz (even at 116 °C) is insufficient to completely average the residual homonuclear ^{1}H−^{1}H dipolar coupling which clearly makes a dominating contribution to the fwhm in the ^{1}H MAS spectra.

Thermal Analysis. To explore the physical properties of the anion-substituted material $Li(BH_4)_{0.91}Cl_{0.09}$, (s1), simultaneous thermogravimetry (TGA) and differential scanning calorimetry (DSC) have been conducted. A continuous experiment with three heating and cooling cycles have been performed shortly after the in situ SR-PXD cycle experiment (see Figure 2) and the initial sample composition is $Li(BH_4)_{0.91}Cl_{0.09}$. During the first heating, the phase transition from *o*- to *h*-$Li(BH_4)_{0.91}Cl_{0.09}$ is seen at 104 °C, which is about 10 °C lower as compared to pure $LiBH_4$ (Figure 10). The TG data is not shown, because no mass loss is observed during the measurements. During cooling of the sample, no DSC signal is observed for the phase transition from *h*- to *o*-$Li(BH_4)_{1-x}Cl_x$ ($x \sim 0.42$) (data not shown). This supports the results from the in situ SR-PXD experiments, which demonstrate that the phase transition temperature (during cooling) when a high quantity of Cl^- is substituted, is at approximately 20 °C. Nevertheless, a small amount of *h*-$Li(BH_4)_{0.58}Cl_{0.42}$ must slowly change into *o*-$Li(BH_4)_{0.58}Cl_{0.42}$, due to the small signal observed at 98 °C during the second and third heating cycle. The lower phase transition temperature indicates that more Cl^- has been substituted into the structure. Interestingly, the melting point of the substituted sample (first heating) is not observed until 297 °C, which is 17 °C higher as compared to that of pure $LiBH_4$. This illustrates a stabilization of the hexagonal phase. For the second and third heating cycles the melting is detected at almost the same temperatures as for the first heating. This shows that the additional substitution of the Cl^-, which was also observed by the in situ SR-PXD experiment, occurs quite rapidly and before reaching the melting point. The signal from the melting point is slightly broadened due to a range of different sample compositions, with slightly different melting points. These changes in temperatures for the phase transition and melting indicate a stabilization of the hexagonal phase caused by the incorporation of Cl^- in the $LiBH_4$ structure. Furthermore, these data confirm that the additional substitution, which occurs during heating, is a fast reaction.

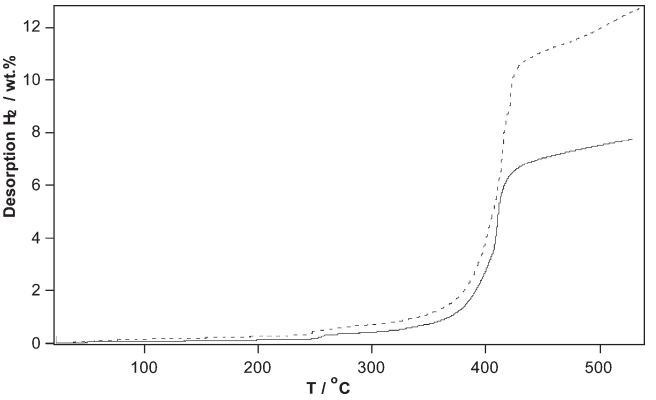

Figure 11. TPD curve for two samples $LiBH_4$ (dashed line) and $Li(BH_4)_{0.77}Cl_{0.23}$ (solid line) found in $LiBH_4$−LiCl (1:1, s1) (solid).

Temperature Programmed Desorption (TPD). TPD measurements have been conducted to study the decomposition of the $Li(BH_4)_{1-x}Cl_x$ (x is approximately 0.23 following 4 months after the preparation) and $LiBH_4$ samples (Figure 11). For both samples, only a tiny quantity of hydrogen is desorbed from RT to 225 °C. A minor hydrogen release in the temperature range from 50 to 100 °C is often observed which most likely is due to adsorbed water forming a small amount

(46) Corey, R. L.; Shane, D. T.; Bowman, R. C.; Conradi, M. S. *J. Phys. Chem. C.* **2008**, *112*, 18706–18710.
(47) Skripov, A. V.; Solonini, A. V.; Filinchuk, Y; Chernyshov, D. *J. Phys. Chem. C.* **2008**, *112*, 18701–18705.

of $LiBH_4 \cdot H_2O$.[48,21] The main desorption of hydrogen occurs for $T > 300$ °C where the two samples show similar kinetics. The TPD measurements are terminated at 550 °C where a slow desorption of hydrogen occurs, and therefore, the total weight loss is slightly underestimated. The samples $Li(BH_4)_{0.77}Cl_{0.23}$ (s1) and $LiBH_4$ release 7.7 and 12.7 wt % hydrogen, respectively. This is in good agreement with the calculated mass loss of 8.9 and 13.9 wt %, assuming that the samples decompose to mixtures of LiH, LiCl, and B. The samples therefore desorbed 87 and 91% of the maximum capacity, respectively, for the substituted and pure sample. This shows that the presence of LiCl in the $LiBH_4$ melt has a minor retarding effect on the hydrogen desorption.

4. Conclusion

An approach to tailor hydrogen storage properties by anion substitution in borohydride based materials is reported. From a combined SR-PXD and MAS NMR experimental study, the structural and physical information on chloride substitution in $LiBH_4$ as a function of temperature and time is revealed. It was found that LiCl readily dissolves in the structure of *h*-$LiBH_4$ upon heating mixtures of $LiBH_4$−LiCl to temperature above the temperature for the phase transition *o*- to *h*-$LiBH_4$. Chloride substitution for BH_4^- in $LiBH_4$ strongly influences the phase transition temperature upon cooling, and *h*-$Li(BH_4)_{1-x}Cl_x$ can be stabilized at RT. On the other hand, segregation of LiCl from *h*-$Li(BH_4)_{1-x}Cl_x$ is found to be a slow process, and the hexagonal compound will slowly revert to an orthorhombic structure *o*-$Li(BH_4)_{1-x}Cl_x$ with a lower chloride content. Rietveld refinement of powder X-ray diffraction data measured for chloride substituted samples reveal a composition of *o*-$Li(BH_4)_{0.91}Cl_{0.09}$ left 13 months at RT and *h*-$Li(BH_4)_{0.58}Cl_{0.42}$ at $T = 224$ °C. Chloride substitution in $LiBH_4$ has a significant influence on the unit cell parameters. Solid-state ^7Li, ^{11}B, and ^1H VT MAS NMR was utilized in order to gain information about the dynamic properties of $LiBH_4$ and $Li(BH_4)_{1-x}Cl_x$. An increase in fwhm for the central resonance was observed when approaching the phase transition, which is reduced by more than a factor of 10 following the phase transition from *o*- to *h*-$LiBH_4$. Thermal analysis further demonstrated the stabilization of the hexagonal phase in $Li(BH_4)_{1-x}Cl_x$, and the temperature programmed desorption measurement shows a minor stabilization of the hydrogenated state and desorption of hydrogen at slightly higher temperatures compared to pure $LiBH_4$. On the other hand, this may facilitate hydrogenation of the $LiBH_4$−LiCl systems as compared to $LiBH_4$, which is also recognized as a serious drawback for the utilization of $LiBH_4$ based systems. In fact, this observation is in accordance with previous studies of the systems $LiBH_4-MgB_2-TiCl_3$ and $LiBH_4-CaH_2-TiCl_3$, where rehydrogenation occurred at relatively moderate conditions.[17,41] It was recently shown that ball milling lead to the formation and decomposition of $Ti(BH_4)_3$ and a residue of solid LiCl,[49] which may facilitate hydrogen uptake.

Recently, anion substitution is also suggested to improve ion conductivity, which is crucial for battery technology. The fast Li^+ conductivity in the hexagonal phase and the stabilization of this phase at RT could make $Li(BH_4)_{1-x}Cl_x$ interesting for use in lithium ion batteries.[40,50,51] However, this study reveals that the composition of substituted systems may change over time, e.g. a reduction of the temperature may lead to a slow segregation of LiCl from $LiBH_4$−LiCl, which will modify the ion conductivity properties. Anion substitution with larger ions, e.g., $Br^- \rightarrow BH_4^-$, smaller ions, e.g., $F^- \rightarrow H^-$, or more than one type of ions may have other effects to be explored in the future.

Acknowledgment. The work at BNL was supported by the US DOE under contract DE-AC02-98CH10886. We are grateful for financial support from the Danish research councils, their research centre *Danscatt*, and the Carlsberg Foundation. The EU is thanked for the grant (no. 226943) *FlyHy* financed via EU-FP7.

Supporting Information Available: Calculated intensity and difference plots for the refinements, crystal data, structural refinement parameters, and ^7Li MAS NMR spectra of the substituted sample. This material is available free of charge via the Internet at http://pubs.acs.org.

(48) Filinchuk, Y.; Chernyshov, D.; Nevidomskyy, A.; Dmitriev, V. Destabilization of light borohydrides by pressure, temperature and by reaction with water. Presented at MH2008 International Symposium on Metal-Hydrogen Systems, Reykjavik, Iceland, June 24−28, **2008**.

(49) Fang, Z. Z.; Ma, L. P.; Kang, X. D.; Wang, P. J.; Wang, P.; Cheng, H. M. *Appl. Phys. Lett.* **2009**, *94*, 044104.

(50) Tarascon, J. M; Armand, M *Nature* **2001**, *414*, 359–367.

(51) Armand, M; Tarascon, J. M *Nature* **2008**, *451*, 652–657.